Position/Force Hybrid Control of a Manipulator with a Flexible Tool Using Visual and Force Information

Jian Huang, Isao Todo & Tetsuro Yabuta

1. Introduction

1.1 Background

Robots used for industrial applications such as welding, painting and object handling have been common for many years. In recent years, the development of domestic robots has become more and more important because of the large and growing population of aged people, especially in Japan. To assist people in their daily lives, a robot must have the ability to deal with not only rigid objects but also the deformable and fragile objects usually encountered in our daily life. Many control algorithms have been developed for the manipulation of rigid objects, and in the recent past many studies related to robotic manipulation of deformable objects have also been reported (Hirai, 1998).

1.2 Recent Researches on Manipulating Deformable Objects

In recent years, the robotic manipulation of flexible objects has been demonstrated in a variety of applications. Manipulation of a deformable tube based on human demonstration (Hirai & Noguchi, 1997), wire manipulation (Nakagaki et al., 1997, Nakagaki, 1998), a study of manipulating a linear objects (Remde et al., 1999, Acker & Henrich, 2003, Schlechter & Henrich, 2002, Schmidt & Henrich, 2001, Yue & Henrich, 2002), one-handed knotting manipulation (Wakamatsu et al., 2002, 2004), handling of fabric objects (Ono, 1998), ticket handling (Itakura, 1998) and contact task on a flexible plate (Wu, et. al., 1997) have been developed,.

In general, deformable objects display a wide range of responses to applied forces because of their different physical properties. Therefore, different control strategies are required for a robot to manipulate different kind of objects. Deformation model analysis is one of the fundamental methods available. Trials have been made of methods based on establishing a deformation model for robot manipulation (Wakamatsu & Wada, 1998, Hisada, 1998), and a state-transition method (Henrich , et. al., 1999, Remde, et al., 1999, Abegg, et al., 2000).

When a human manipulates a deformable object, he will actively combine visual information from his eyes with contact force information obtained by his hands. Vision-based state detection for a linear object (Acker & Henrich, 2003, Abegg, et al., 2000) and visual tracking of a wire deformation (Chen & Zheng, 1992, Nakagaki et al., 1997) have been reported.

Open Access Database www.i-techonline.com

Source: Cutting Edge Robotics, ISBN 3-86611-038-3, pp. 784, ARS/plV, Germany, July 2005 Edited by: Kordic, V.; Lazinica, A. & Merdan, M.

Furthermore, a control method based on high-speed visual detection and visual/force sensor fusion was proposed to enable a robot to complete the task of inserting an aluminum peg held by a manipulator into an acrylic hole fixed on a deformable plate (Huang & Todo, 2001). In a continuing study, a stereovision-based compliance control enabling a robot arm to manipulate an unknown deformable beam object (Huang, et al., 2003) has been demonstrated, in which stereovision and force information were combined by an online learning neural network so that the robot could adjust its position and orientation in response to the deformation state of the unknown beam object.

1.3 Description of the Study in this Chapter

A robot with a flexible tool is considered the first choice for manipulating a fragile object. However, in contrast with the extensive literature on robot manipulation of rigid and deformable objects, the study of how to control a robot arm with a flexible tool has been neglected. Therefore, a great need exists to develop fundamental control methods for robots with flexible tools.

When a robot arm with a flexible tool is used to complete a contact task, deformation of the flexible tool always occurs so that the task can not be adequately completed by using solely the type of control methods designed for a robot with a rigid tool. As the position of the tool's tip can not be computed from the robot's kinematics, establishing a deformation model of the flexible tool is generally needed to estimate the position of the flexible tool's tip.

In this chapter, a position/force hybrid control method that incorporates visual information is proposed to enable a robot arm with a flexible tool to complete a contact task. To detect the position of the flexible tool's tip, two CCD cameras are used and a real time image processing algorithm is developed. Furthermore, an online learning neural network is introduced to the position/force hybrid control loop so as to improve the tracing accuracy of the flexible tool. An advantage of the proposed method is that establishing a deformation model of the flexible tool is not necessary.

With the proposed method, a flexible tool held by the end-effector of a 6 DOF robot is used to trace a given curve with a specified vertical pressing force.

2. Overview of the Robot System

The robot control system considered in this chapter includes a manipulator with seven degrees of freedom (PA-10, Mitsubishi Heavy Industry Co.), a force/torque sensor (10/100, B.L. Autotec Ltd.) for force detection, two compact CCD cameras (XC-EI50, Sony Co.) for stereo visual detection and a personal computer (Dimension XPS B733r, Dell Co.) for algorithm calculation. However, the redundant joint of the manipulator is fixed. A schematic diagram of the robot system is shown in Fig.1.

As shown in Fig.1, a cylindrical tube made from polyvinyl chloride (10.7 mm diameter) is used as the tool, and is held by the end-effector of the manipulator. The tip of the flexible tool is wrapped with a light-reflective tape for image detection. A infrared ring type radiators (IRDR-110, Nissin Electronic Co.) is set up in front of each camera's lens.

The required task is for the flexible tool held by the robot to trace a given curve with a specified pressing force. As deformation of the flexible tool always occurs on contact, control of the flexible tool's tip to make it trace a desired trajectory is very difficult.

In order to estimate the tool's tip position, establishing a deformable model is usually considered.

Figure 1.The schematic diagram of the robot system with a flexible tool

Therefore, some physical parameters like the stiffness and Young's modulus of the flexible tool are needed for model analysis. However, such physical parameters are usually unknown for many of the materials encountered in daily life.

3. Method of Image Processing

3.1 Real Time Image Processing

As shown in Fig.1, two synchronized compact cameras are used to construct a stereovision system. Each camera outputs images at the rate of 30 frames per second. For image input and processing, a graphic board with a C80 digital signal processor (GENESIS GEN/F/64/8 /STD, Matrox Co.) is installed in the personal computer.

Generally, real time image processing means that one frame image from a camera must be processed within the camera's frame time so that image input and processing can be carried out simultaneously. Real time image processing is commonly achieved with parallel processing.

In this chapter, we use a method called double buffering to achieve parallel image processing. As shown in Fig.2, images are successively output from cameras 1 and 2. At times n = 0, 2, 4, ···, new images from cameras 1 and 2 are taken into buffers 11 and 21 respectively, while the last images saved in buffers 12 and 22 are processed. At times n = 1, 3, 5, ···, functions of the buffers are exchanged. Images from cameras 1 and 2 are taken into buffers 12 and 22 respectively, while the last images saved in buffers 11 and 21 are processed.

By using the parallel processing, a stereo image can be processed within the camera frame time T_c (33.33 ms). Therefore, the tool tip's position $\boldsymbol{p}_t(n) \in R^{3\times1}$ (n = 0, 1, 2, ···) in the robot base coordinate Σ_b can be detected at each camera's frame time T_c. Thus, real time image processing is achieved.

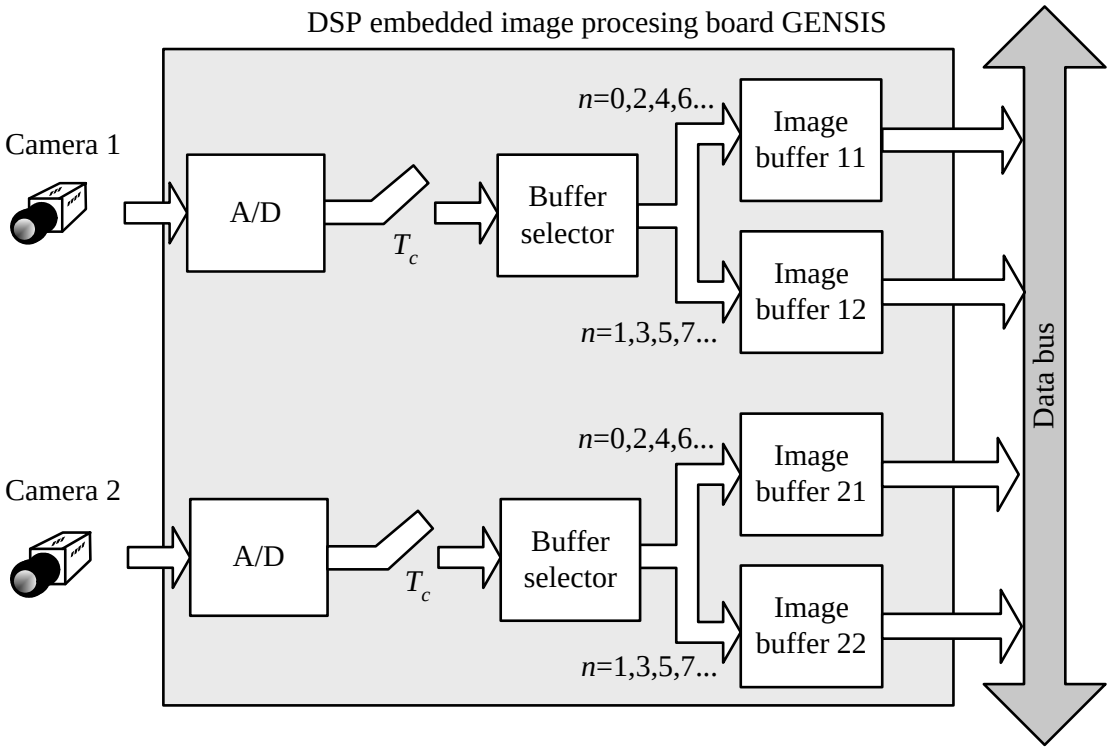

Figure 2. Parallel image processing in GENESIS using double buffering method

3. 2 Interpolation of the Image Detection Results

The robot control sampling period T is 5 milliseconds. At time t = k_T, the position of the flexible tool's tip in the robot base coordinate Σ_b is assumed to be $\boldsymbol{p}_t(k) \in R^{3\times1}$. By using the real time image processing method described in section 3.1, the tool's tip position $\boldsymbol{p}_t(n)$ in Σ_b can be detected within the camera frame time T_c. However, the image processing sampling period T_c is still longer than the robot control sampling period T. A time chart of image processing and robot control is shown in Fig. 3, where T_n (100 ms) is the least common multiple of T_c and T. Therefore, interpolation is necessary to convert the result $\boldsymbol{p}_t(n)$ of image processing to $\boldsymbol{p}_t(k)$ at every sampling period T for robot control. In the period T_n, the position $\boldsymbol{p}_t(k)$ can be calculated by

$$\boldsymbol{p}_t(k) = \begin{cases} \boldsymbol{p}_t(n-1) + (kT-(n-1)T_c)\dfrac{\boldsymbol{p}_t(n-1)-\boldsymbol{p}_t(n-2)}{T_c} \\ \qquad (nT_c \le kT < (n+1)T_c), \\ \boldsymbol{p}_t(n) + (kT-nT_c)\dfrac{\boldsymbol{p}_t(n)-\boldsymbol{p}_t(n-1)}{T_c} \\ \qquad ((n+1)T_c < kT < (n+2)T_c), \\ \boldsymbol{p}_t(n+1) + (kT-(n+1)T_c)\dfrac{\boldsymbol{p}_t(n+1)-\boldsymbol{p}_t(n)}{T_c} \\ \qquad ((n+2)T_c < kT < (n+3)T_c), \\ \cdots\cdots\cdots\cdots\cdots\cdots\cdots\cdots \\ \qquad (k = 0,1,2,\cdots),(n = 0,1,2,\cdots)\ . \end{cases} \tag{1}$$

In equation (1), $\boldsymbol{p}_t(-1)$ and $\boldsymbol{p}_t(-2)$ are set equal to 0 for n = 0.

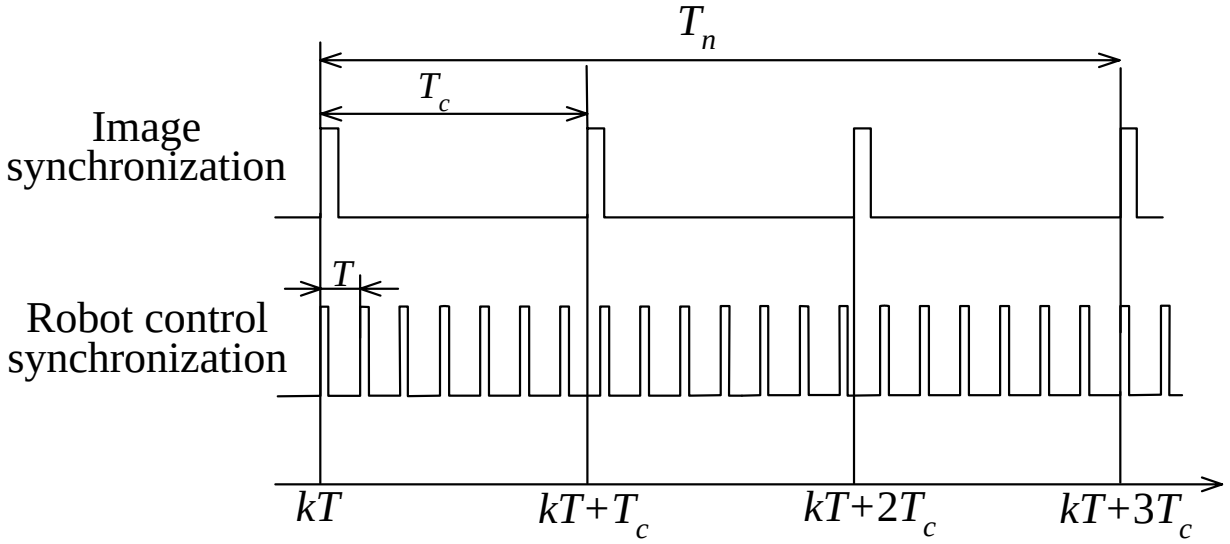

Figure 3. The time chart of image processing and robot control

4. Generation of Desired Trajectory

If a rigid tool held by a manipulator is used to complete the task as shown in Fig.1, the tool will not deform, so the position of the tool's tip can easily be calculated from the kinematics of the manipulator. However, when a flexible tool is used, it deforms on contact so that the position of the tool's tip cannot be directly computed from the kinematics of the manipulator. To explain the principle of the generation of the desired trajectory, a model is assumed as shown in Figs.4 and 5, where the tool's tip moves along the x axis with a constant pressing force in the z direction.

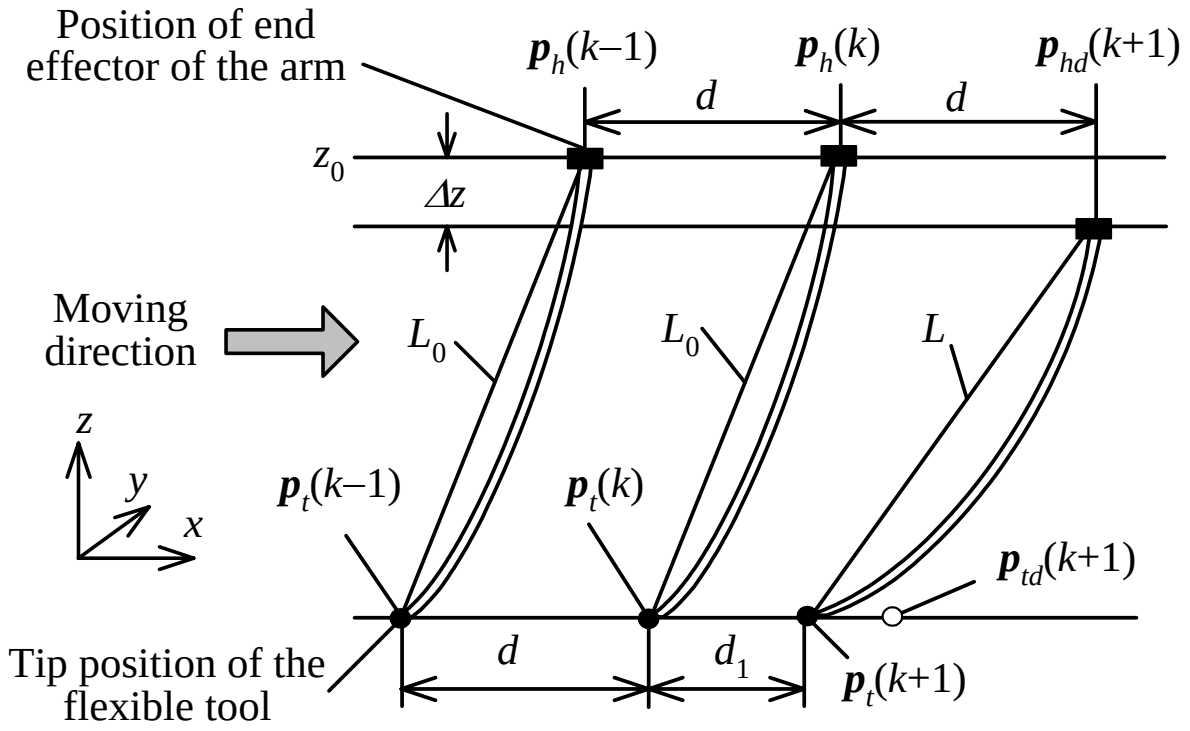

Figure 4. Moving end-effector of the robot forward with a distance d

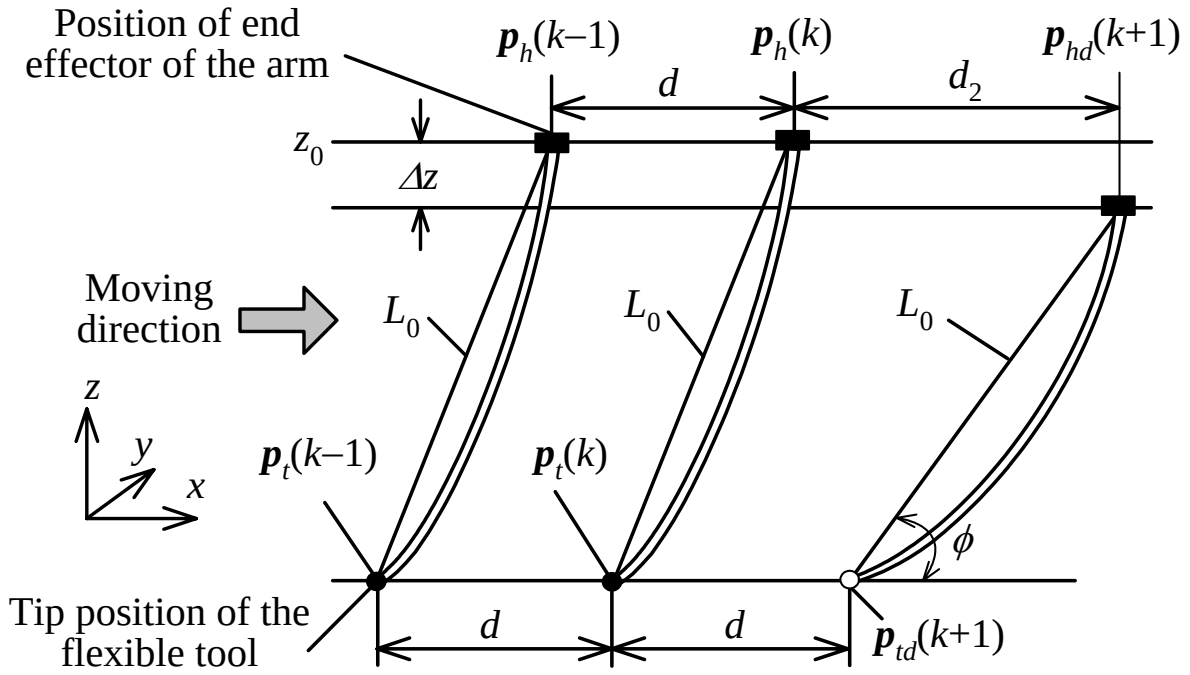

Figure 5. Moving the flexible tool forward with a distance d

Further assumptions of the task are the following:

- The desired trajectory traced by the flexible tool is in a given plane.
- The orientation around the y axis of the end-effector shown in Figs.4 and 5 is kept to be unchanged at its initial value until the task is completed.

4.1 Desired Trajectory Generation of the Robot's End-Effector

At time t = k_T, when the end-effector of the robot moves by a distance d from position $\boldsymbol{p}_{hd}(k) \in R^{3\times1}$ to position $\boldsymbol{p}_{hd}(k+1)$ as shown in Fig.4, the variation Δz along the z axis of the end-effctor caused by deformation will lead to the result that the flexible tool's tip moves by the distance d1 from position $\boldsymbol{p}_t(k) \in R^{3\times1}$ to position $\boldsymbol{p}_t(k+1)$ rather than to the desired position $\boldsymbol{p}_{td}(k+1)$.

As shown in Fig.5, in order to move the tool's tip to the desired position ptd(k+1) ahead of position $\boldsymbol{p}_t(k)$ by the distance d, the end-effector of the arm should be moved by the distance d2 from position ph(k) to position $\boldsymbol{p}_{hd}(k+1)$ to compensate for the position error caused by the variation Δz of the robot end-effector.

Here, we assume that the distance between the tool tip and the end-effector is L0 when the tool presses against the contact surface with a constant force fzd. At time t = kT, the desired position of the tool's tip is expressed as $\boldsymbol{p}_{td}(k+1)=[x_{td}(k+1),\ y_{td}(k+1),\ z_{td}(k+1)]^T$, and the angle between line L_0 and the x-y plane is ϕ. Thus, the moving direction vector $\tilde{\boldsymbol{p}}_{td}(k)$ of the tool's tip can be computed by

$$\tilde{\boldsymbol{p}}_{td}(k) = \frac{\boldsymbol{p}_{td}(k+1) - \boldsymbol{p}_{td}(k)}{d}, \tag{2}$$

where d is given by

$$d = \sqrt{(x_{td}(k+1) - x_{td}(k))^2 + (y_{td}(k+1) - y_{td}(k))^2}. \tag{3}$$

The projection vector $\Delta\boldsymbol{p}_L(k) \in R^{3\times1}$ of the tool on the x-y plane is

$$\Delta\boldsymbol{p}_L(k) = L_0 \cos(\phi) \cdot \tilde{\boldsymbol{p}}_{td}(k), \tag{4}$$

where angle Φ can be calculated by

$$\phi = \sin^{-1}\left(\frac{z_0 - \Delta z}{L_0}\right) \tag{5}$$

If the position error $\Delta\boldsymbol{p}_t(k)$ of the tool's tip is considered, the end-effector's desired position in the x-y plane is given by

$$\boldsymbol{p}_{hd}^{xy}(k) = \boldsymbol{p}_{td}(k+1) + \Delta\boldsymbol{p}_L(k) + \Delta\boldsymbol{p}_t(k), \tag{6}$$

Therefore, the desired position phd(k) of the end-effector is generated by

$$\boldsymbol{p}_{hd}(k+1) = \boldsymbol{S}_1 \cdot \boldsymbol{p}_{hd}^{xy}(k) + z_d \cdot \boldsymbol{s}_1, \tag{7}$$

where zd is equal to the initial coordinate z0, and matrix S1 and vector s1 are given by

$$\boldsymbol{S}_1 = \begin{bmatrix} 1 & 0 & 0 \\ 0 & 1 & 0 \\ 0 & 0 & 0 \end{bmatrix}, \tag{8}$$

$$\boldsymbol{s}_1 = [0 \quad 0 \quad 1]^T. \tag{9}$$

4.2 Desired Orientation of the Arm's End-Effector

At time t = kT, the desired orientation of the end-effector is expressed as

$$\boldsymbol{r}_{hd}(k) = [\alpha_d(k) \quad \beta_d(k) \quad \gamma_d(k)]^T, \tag{10}$$

where αd(k), βd(k) and γ d(k) are the rotation angle of the end-effector around the xb axis, yb axis and zb axis respectively, defined by the x-y-z fixed-angle method. If the end-effector pushes the tool to move along the desired curve as shown in Fig.6, a twisting moment will cause the rotation of the tool so that the tool's tip position will be uncontrollable.

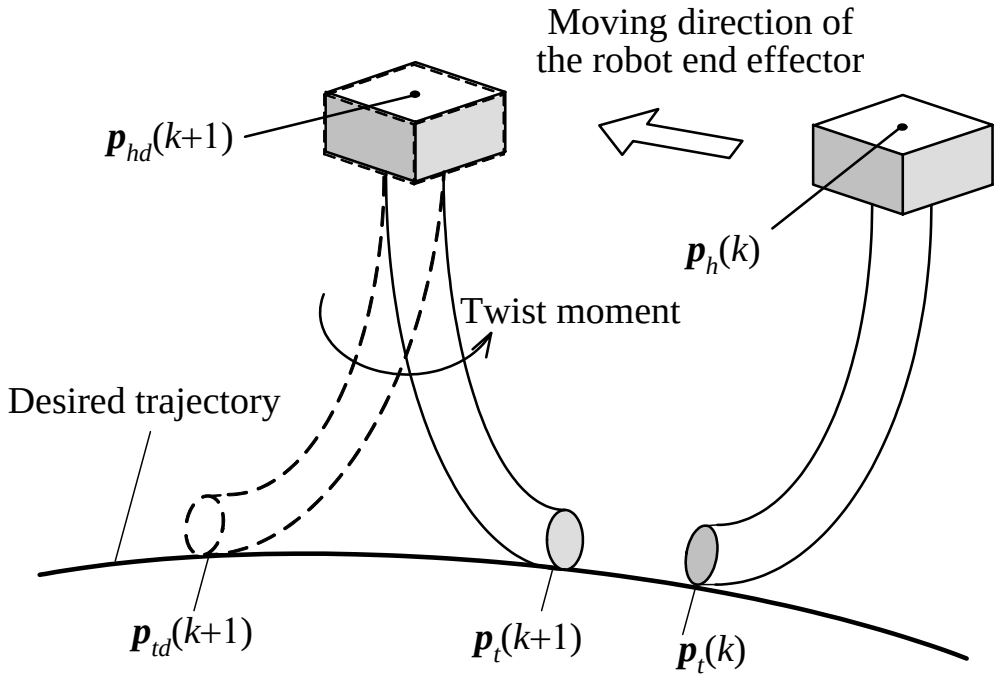

Figure 6. Rotation of the flexible tool caused by twist moment

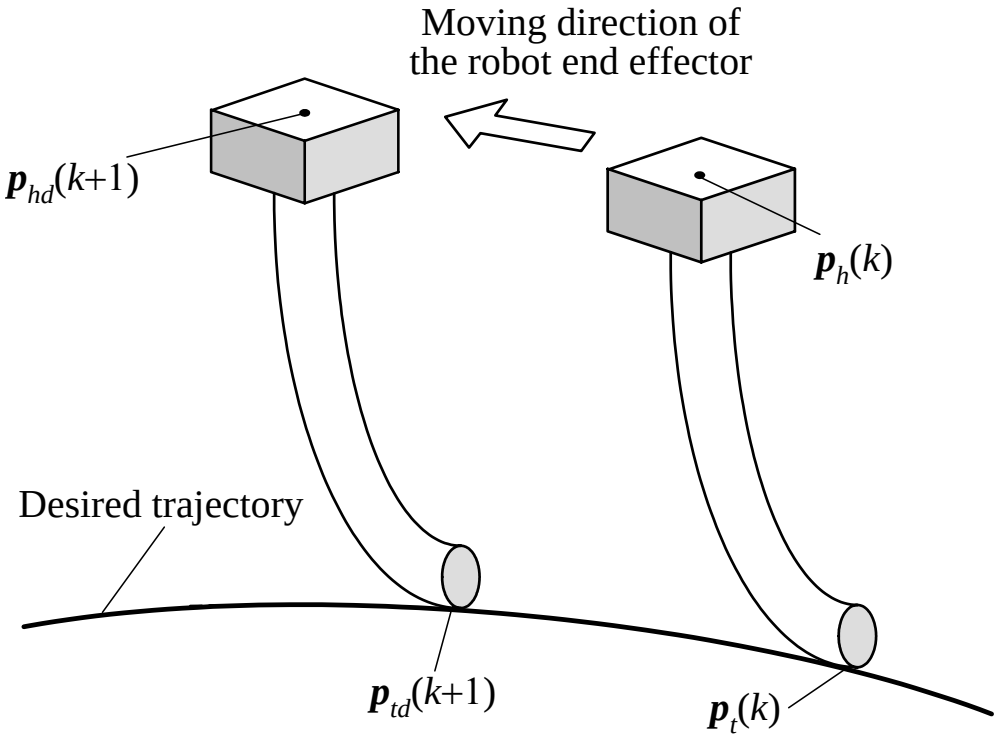

Figure 7. Rotation avoidance by pulling the flexible tool

In order to avoid rotation of the tool, a method of pulling the flexible tool with the end-effector is determined as shown in Fig.7. Therefore, the desired orientation of the end-effector is computed by

$$\boldsymbol{r}_{hd}(k) = [\alpha_d \quad \beta_d \quad \tan^{-1}(\frac{y_{td}(k)}{x_{td}(k)})]^T \tag{11}$$

Then, by equations (7) and (11), the desired position and orientation prd(k+1)□□R6×1 of the end-effector can be calculated by

$$\boldsymbol{p}_{rd}(k+1) = \boldsymbol{S}_p \cdot \boldsymbol{p}_{hd}(k) + \boldsymbol{S}_r \cdot \boldsymbol{r}_{hd}(k), \tag{12}$$

where

$$\boldsymbol{S}_p = \begin{bmatrix} 1 & 0 & 0 \\ 0 & 1 & 0 \\ 0 & 0 & 1 \\ 0 & 0 & 0 \\ 0 & 0 & 0 \\ 0 & 0 & 0 \end{bmatrix}, \qquad \boldsymbol{S}_r = \begin{bmatrix} 0 & 0 & 0 \\ 0 & 0 & 0 \\ 0 & 0 & 0 \\ 1 & 0 & 0 \\ 0 & 1 & 0 \\ 0 & 0 & 1 \end{bmatrix}.$$

4.3 Desired Pressing Force

As a constant force is required for the tip of the flexible tool to press the contact surface, the desired force f(k) is determined by

$$\boldsymbol{f}(k) = \begin{bmatrix} 0 & 0 & f_{zd} \end{bmatrix}^T, \tag{12}$$

where fzd is the constant force along the zb axis. If the end-effector pushes the tool as shown in Fig.6, a large pressing force acting between the tool's tip and the contact surface will increase friction so as to easily bring about rotation of the tool caused by the twist moment.

5. Hybrid Control Algorithm

5.1 Online Learning Neural Network

To complete the required task, position control in the xb-yb plane and force control along the zb axis are considered. However, unspecified factors such as friction at the tool's tip and deformation of the tool will impair the tracing accuracy of the tool.

To improve the tracing accuracy of the tool's tip in the xb-yb plane, two online learning neural networks are introduced, one each for the x and y directions as shown in Fig.8. For the neural network NNx, the desired position xhd(k), desired velocity $\dot{x}_{hd}(k)$ and desired acceleration $\ddot{x}_{hd}(k)$ are used as the input quantities. Just as in the NNx, the desired position yhd(k), desired velocity $\dot{y}_{hd}(k)$ and desired acceleration $\ddot{y}_{hd}(k)$ are used as the input quantities for the neural network NNy. The position errors of Δxr(k) on the xb axis and Δyr(k) on the yb axis are used as error signals for the neural network's learning.

The neural networks NNx and NNy have same 3-layer structure. The neurons in the input layer, hidden layer and output layer are designated NA, NB and NC respectively. The sigmoid function F(x) is given as

$$F(x)=\frac{1-e^{-x/\mu}}{1+e^{-x/\mu}}, \tag{13}$$

where μ is the annealing parameter. Learning of the weighting coefficients is obtained with back propagation method [Cichocki & Unbehauen, 1993].

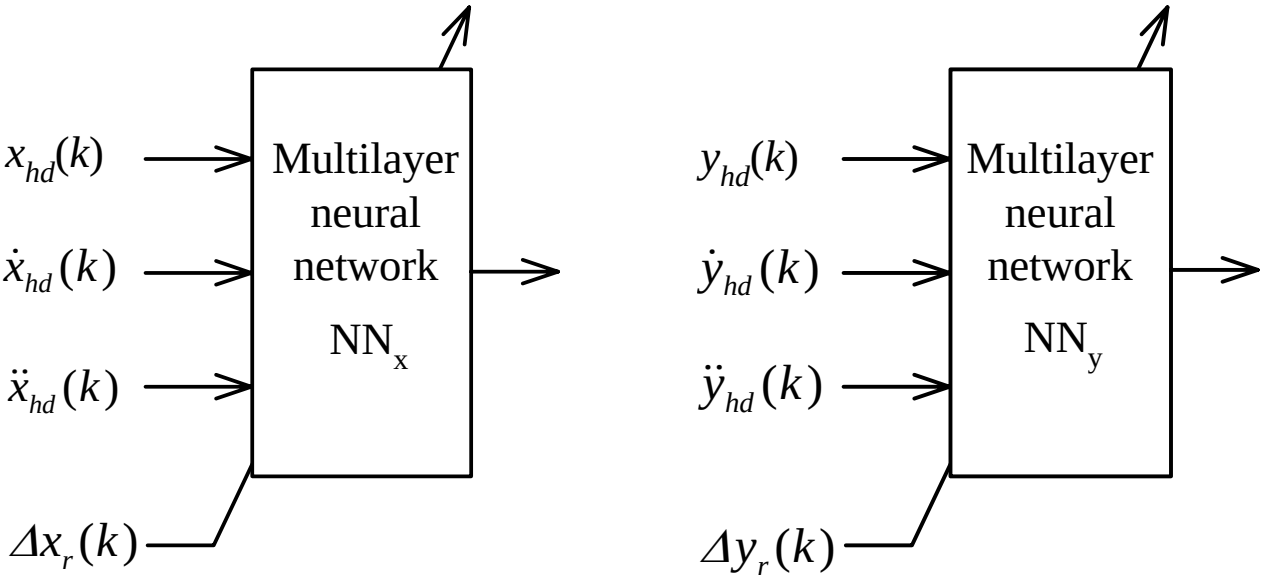

Figure 8. The proposed online learning neural networks

5.2 The Proposed Hybrid Control Method

A position/force hybrid control method using two online learning neural networks is proposed to enable a robot with a flexible tool to trace a given curve. The control block diagram is shown in Fig.9, where Λ is the kinematics, J is the Jacobian and Rf is the rotation matrix for calculating fz from fenv(k) detected by the force/torque sensor.
Matrix S2 and vector sf are given as

$$\boldsymbol{S}_2=\begin{bmatrix}1&0&0&0&0&0\\0&1&0&0&0&0\end{bmatrix}, \qquad \boldsymbol{s}_f=\begin{bmatrix}0&0&1&0&0&0\end{bmatrix}^T$$

The PID controller Gp(z) of the position loop is networks

$$\boldsymbol{G}_p(z)=\boldsymbol{K}_P^p+\boldsymbol{K}_I^p\frac{z}{z-1}+\boldsymbol{K}_D^p(1-z^{-1}), \tag{14}$$

and the PID controller Gf(z) of the force loop is

$$G_f(z)=K_P^f+K_I^f\frac{z}{z-1}+K_D^f(1-z^{-1}) \tag{15}$$

For the position control loop in Fig.9, at time t = kT, interpolation is made by equation (1) for the image detection result p(n−1) so as to obtain the tool tip's position pt(k). After the projection of the vector ΔpL(k) on the x-y plane is calculated with equation (4), the desired position phd(k) can be generated by equation (7). Thus, the desired position and orientation prd(k) are computed by equation (12).
Position errors between the desired position prd(k) and the present position pr(k) calculated from the kinematics are used as error signals for the neural network's learning.

Figure 9. The proposed position/force hybrid control algorithm with using the online learning

For the force control loop, the desired force fzd and the contact force fz in the z directrion are compared, and the force error is input to the PID controller Gf(z).

Then, the desired joint velocity $\dot{\boldsymbol{\theta}}_d(k)$ is computed by using the inverse of Jacobian J and is input to the servo driver of the manipulator.

6. Experiments and Discussion

Several experiments have been performed to prove the effectiveness of the proposed method as shown in Fig.9. The control parameters used in the experiments are given in Table 1.

$\boldsymbol{K}_P^p = \mathrm{diag}[K_{P1}^p \quad K_{P1}^p \quad 0 \quad K_{P2}^p \quad K_{P2}^p \quad K_{P2}^p]$
K_{P1}^p=5.01/s, K_{P2}^p=2.01/s
$\boldsymbol{K}_I^p = \mathrm{diag}[K_{I1}^p \quad K_{I1}^p \quad 0 \quad K_{I2}^p \quad K_{I2}^p \quad K_{I2}^p]$
K_{I1}^p=0.51/s, K_{I2}^p=0.21/s
$\boldsymbol{K}_D^p = \mathrm{diag}[K_{D1}^p \quad K_{D1}^p \quad 0 \quad K_{D2}^p \quad K_{D2}^p \quad K_{D2}^p]$
K_{D1}^p=0.11/s, K_{D2}^p=0.11/s
K_P^f=0.001 m/(s·N), K_I^f=0.0005 m/(s·N), K_D^f=0.0001 m/(s·N)

Table 1. Control parameters used in the experiments

6.1 Influences on Tracing Accuracy of the Tool Caused by Twist Moment (Without Applying Neural Networks and Orientation Control)

A circular trajectory is given in Fig.10. The radius R of the circle is 0.1 meters. In order to investigate the influence of twist moments on the flexible tool, position control is imposed on the end-effector, while the orientation of the end-effector is fixed at its initial value. In this experiment, the stereovision detection and neural networks described in Fig.9 are not used.

Other parameters used are as follows.

For position/orientation control:z_d=0.750,αd=0, β_d=1.222 rad, γ_d=0.

For force control:fzd = 2 N.

Results for the end-effector's position ph(k) and the tool's tip position pt(k) are shown in Fig.11. Because the tool's deformation is not considered, a position error in the starting point caused by deformation of the flexible tool is observed in Fig.11. On the path through points p_0, p_1 and p_2 as shown in Fig.11, the tool's tip follows the movement of the end-effector but a large position error is generated. Rotation of the flexible tool caused by a twist moment is not encountered on this route because the flexible tool is pulled by the end-effector. However, on the path along points p_2, p_3 and p_0, the end-effector pushes the flexible tool, so that a twist moment causes rotation of the tool. As a result, the tool's tip is uncontrollable. The above results demonstrate that the tool's deformation and the effect of the twist moment must be considered.

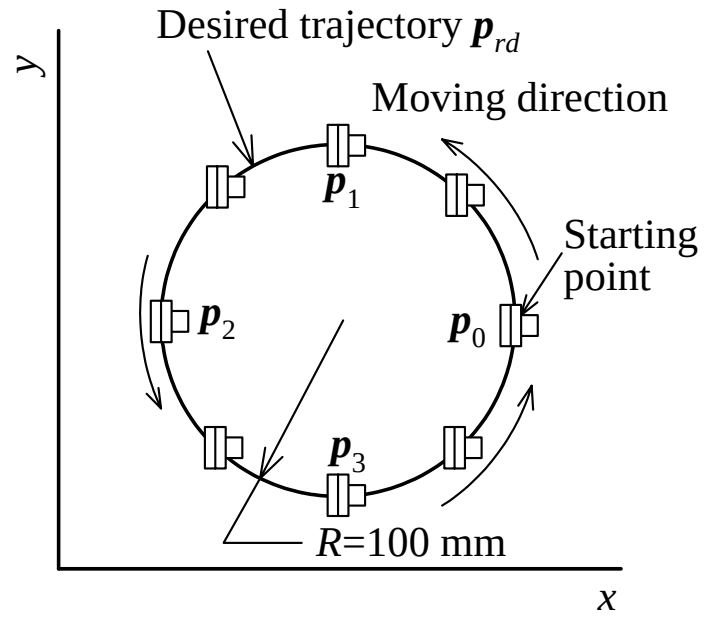

Figure 10. Desired trajectory of the tool's tip

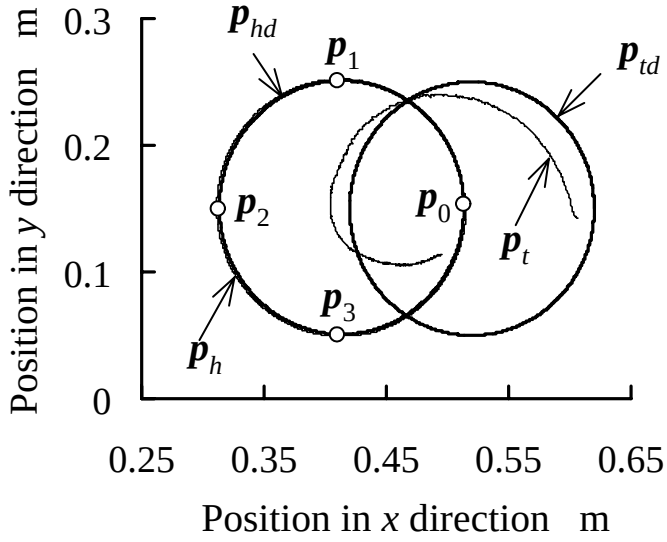

Figure 11. The tool's tip position p_t and end-effector's position p_h

6.2 Tracing Experiment (Without Using Neural Networks)

In order to avoid twist-moment-induced rotation of the flexible tool, it is pulled by the end-effector to trace the desired trajectory as shown in Fig.7. However, due to the arm's mechanical structure, the end-effector can not rotate 360 degrees to trace the circular trajectory shown in Fig.10. Therefore, a sinusoidal curve is given as the desired trajectory in Fig.12. In this experiment, stereovision detection by real time image processing is used, but the neural networks described in Fig.9 are not included in position control. Other parameters are used as follows.

For position/orientation control:zd=0.690,αd=0, βd=1.047 rad.

For force control:fzd = 0.5 N.

The end-effector's position ph(k) and the tool's tip position pt(k) are shown in Fig.13. Compared with the results shown in Fig.11, the tool's tip traces the desired sinusoidal curve with the movement of the end-effector. Furthermore, rotation of the flexible tool caused by the twist moment is successfully avoided by the proposed motion control of the end-effector

as shown in Fig.7. However, in Fig.13, the maximum position error between tool tip's position pt(k) and the desired trajectory ptd(k) along the x axis is 8 mm, and the maximum position error between ptd(k) and pt(k) along the y axis is 12 mm.

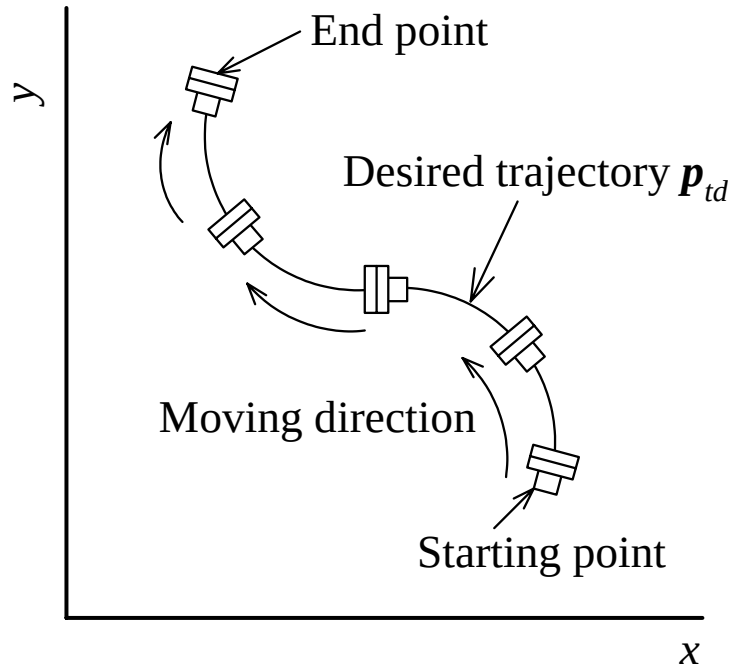

Figure 12. Desired trajectory of the tool's tip

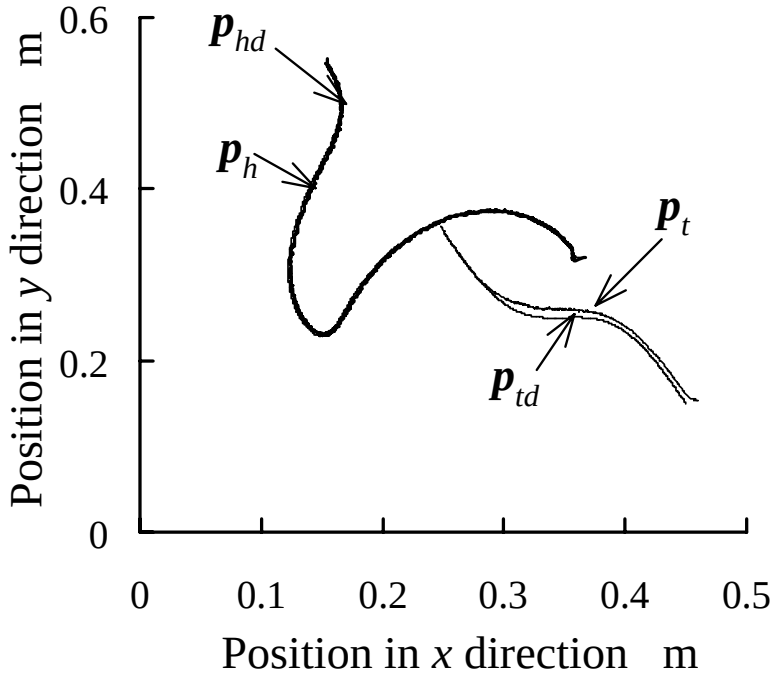

Figure 13. The tool tip's position pt and end effector's position p_h

6.3 Tracing Experiment Using the Proposed Method

In order to improve the tracing accuracy of the flexible tool, the proposed control method using online neural network learning is applied. The desired trajectory is same sinusoidal curve as shown in Fig.12. Other parameters are as follows.

For position/orientation control:zd=0.690,αd=0, βd=1.047 rad.
For force control:fzd = 0.5 N.
The following parameters are used for the proposed neural networks.
Neuron number in the input layer NA= 3.
Neuron number in the hidden layer NB= 6.
Neuron number in the output layer NA= 1.
Annealing rate μ = 1.0.
Learning rate η = 0.85.
The initial values of weighting coefficients of the neural networks are set randomly, and all weighting coefficients are saved in a file for continued learning in the next tracing. It is known that a number of trials are generally needed before the learning error converges [Liu & Todo, 1991]. Results of the error signals for the neural network's learning are shown in Fig.14, where the learning errors settled near zero at the end of the first tracing after 10,000 trials. Furthermore, compared with the error obtained in the first tracing, the tracing accuracy is obviously improved in the second tracing.

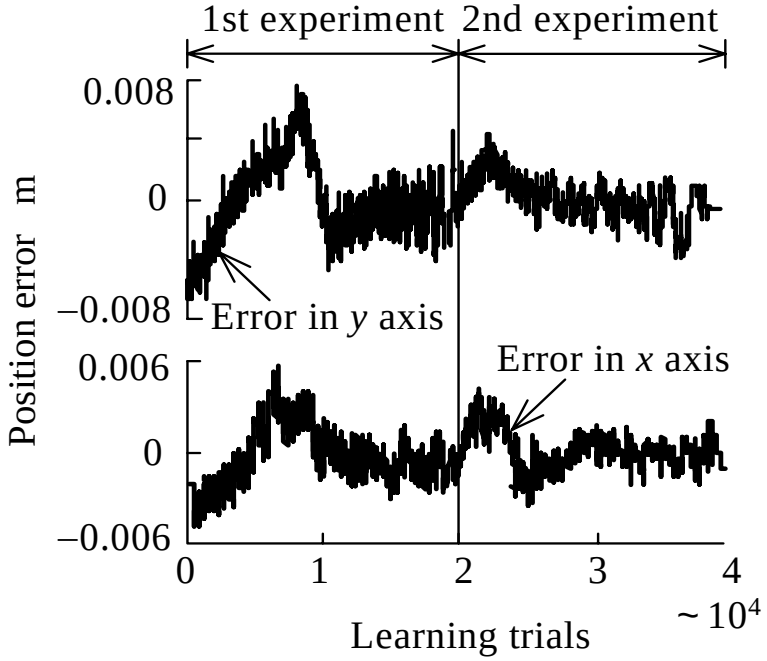

Figure 14. The error signals for neural network learning

The tracing trajectories of the tool's tip and the end-effector's position in the x-y plane are shown in Fig.15, and result of the forces fz is shown in Fig.16. Compared with the results shown in Fig.12, the tracing accuracy of the tool's tip is greatly improved. The maximum position errors between ptd(k) and pt(k) on both the x and y axes are decreased to 4 mm, which is almost half of the error in the experiment without neural networks. Furthermore, the contact force between the tool's tip and the surface is accurately controlled at the desired force fzd.

7. Conclusions and Future Work

For robotic manipulation of a fragile object, using a flexible tool fixed to a robot arm is the obvious choice. However, a flexible tool deforms on contact and control of the flexible tool is difficult because the position of the tool's tip cannot be calculated from the kinematics of the robot arm. We have developed a new approach that is not based on establishing a

deformation model to calculate the tool tip's position, but that uses real time image processing with stereovision. Furthermore, an interpolation algorithm is proposed to convert the image-processing results detected in each camera frame time to the results used at every sampling period for robot control.
Visual detection is a convenient and effective way to obtain information on a deformable object with unknown parameters, which is generally required for deformation model analysis.

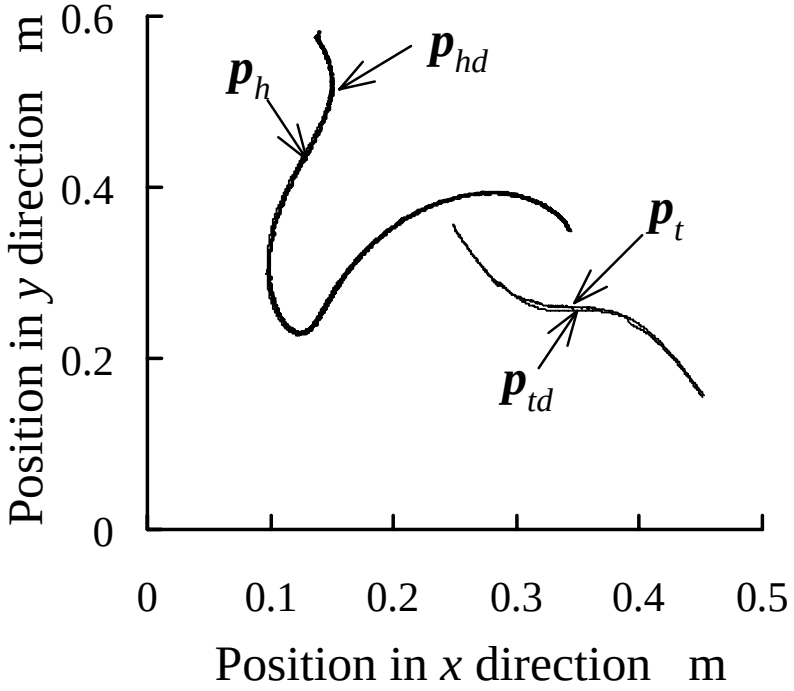

Figure 15. The tool's tip position pt and end effector's position p_h

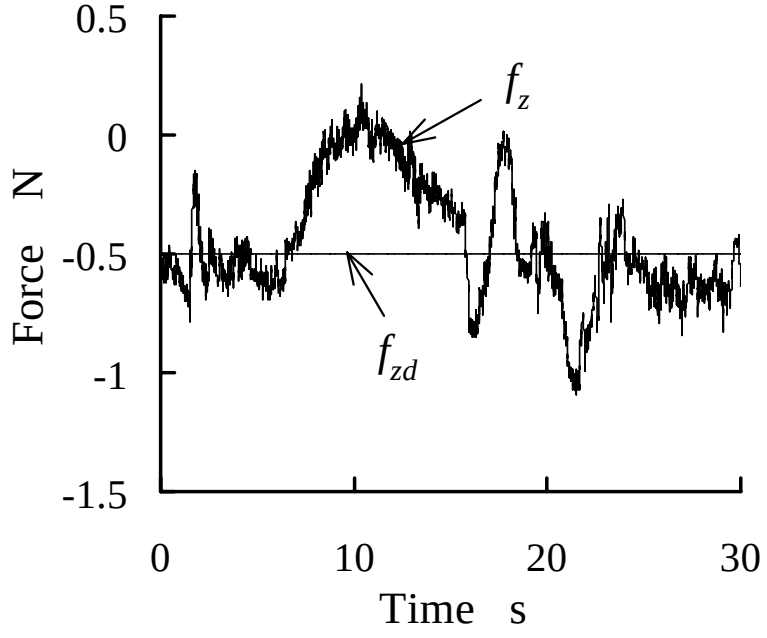

Figure 16. The force results

As shown in Fig.6, control of the deformable tool is difficult because twist moment will cause a rotation of the tool's body so that position of the tool is uncontrollable. Therefore, pulling the flexible tool by the end-effector is considered. In this chapter, a position and force hybrid control method using visual and force information is proposed to enable a flexible tool held by a manipulator to trace a specified curve in a plane. To improve tracing accuracy, online learning neural networks are introduced to construct a feed-forward controller so that the position error of the tool's tip is decreased. The proposed method is used for a manipulator with a flexible tool to trace a sinusoidal curve and it effectiveness is experimentally demonstrated.

For future work, the influence of the pressing force and the physical characteristics of the contact surface will be investigated. In this chapter, a method of avoiding tool rotation caused by the twist moment is proposed. In practice, because the friction coefficients of the contact surfaces vary greatly, any torque can easily cause rotation of the flexible tool. Therefore, a control strategy should be developed to adjust the end-effector's orientation when rotation of the tool occurs. To achieve this control, the visual detection will first be improved by using a number of feature points on the tool body so as to obtain its deformation state. A control algorithm for the end-effector of the arm is also needed for adequate adjustment of the flexible tool.

8. References

Acker, J. & Henrich, D. (2003). Manipulating deformable linear objects: characteristic features for vision-based detection of contact state transitions, Proc. IEEE Int. Symp. on Assembly and Task Planning, pp.204–209, July 10-11, 2003

Abegg, F.; Remde, A. & Henrich, D. (2000). Force and vision based detection of contact state transition, Robot manipulation of deformable objects, Springer, ISBN 1852332506

Cichocki, A. & Unbehauen, R. (1993). Neural networks for optimization and signalprocessing, John Wiley & Sons ISBN 0471930105,

Chen, C. Y. & Zheng,Y. F. (1992). Deformation identification and estimation of one-dimension objects by vision sensors, Journal of Robotic Systems, Vol.9, No.5, pp.595-612

Henrich, D.; Ogasawara, T. & Worn, H. M. (1999). Manipulating deformable linear objects -Contact states and point contacts-, Proc. IEEE Int. Symp. on Assembly and Task Planning, pp.198 - 204, July 21-24, 1999

Hirai, S. (1998). Deformable object manipulation, J. of the Robotics Society of Japan, Vol.16, No.2, pp.136-139

Hirai, S. & Noguchi, H. (1997). Human-demonstration based approach to the object motion design and the recognition of process state transitions in insertion of deformable tubes, J. of the Robotics Society of Japan, Vol.18, No.8, pp.1172-1179

Hisada, T. (1998). Finite element modeling, J. of the Robotics Society of Japan, Vol.16, No.2, pp.140-144

Huang, J. & Todo, I. (2001). Control of a robot based on fusion of visual and force/torque sensor information (Manipulation of a deformable object), Trans. Japan. Soc. Mech. Eng., Series C, Vol.67, No.660, pp.2616-2623

Huang, J.; Todo, I. & Muramatsu, I. (2003). Neuro-control of a robot using visual and force/torque sensor information (Manipulation of a flexible beam object), Trans. Japan. Soc. Mech. Eng., Series C, Vol.69, No.684, pp.2085-2092

Itakura, O. (1998). Manipulation of paper material – ticket handling in station business machine –, J. of the Robotics Society of Japan, Vol.16, No.2, pp.154-158

Liu, M. H. & Todo, I. (1991). Digital control of servo systems using neural networks (A method of off-line learning), Trans. Japan. Soc. Mech. Eng., Series C, Vol.57, No.539, pp.2256-2262

Nakagaki, H. (1998). Insertion task of a flexible beam or a flexible wire, Journal of the Robotics Society of Japan, Vol.16, No.2, pp.159-162

Nakagaki, H.; Kitagaki, K.; Ogasawara, T. & Tsukune, H. (1997). Estimation of a force acting on a flexible wire by using visual tracking and its application to insertion task, J. of the Robotics Society of Japan, Vol.15, No.3, pp.422-430

Ono, E. (1998). Fabric Manipulation, J. of the Robotics Society of Japan, Vol.16, No.2, pp.149-153

Remde, A.; Henrich, D. & Wom, H. (1999). Manipulating deformable linear objects-contact state transitions and transition conditions, Proc. IEEE/RSJ Int. Conf. on Intelligent Robots and Systems,Vol.3, pp.1450-1455, Oct.17-21,1999

Schlechter, A. & Henrich, D. (2002). Manipulating deformable linear objects: manipulation skill for active damping of oscillations, Proc. IEEE/RSJ Int. Conf. on Intelligent Robots and System, Vol.2, pp.1541-1546, Sept.30-Oct.5, 2002

Schmidt, T. W. & Henrich, D. (2001). Manipulating deformable linear objects: robot motions in single and multiple contact points, Proc. IEEE Int. Symp. on Assembly and Task Planning, pp.435-441, May 28-29, 2001

Wakamatsu, H. & Wada, T. (1998). Modeling of string object for their manipulation, J. of the Robotics Society of Japan, Vol.16, No.2, pp.145-148

Wakamatsu, H.; Tanaka, Y.; Tsumaya, A.; Shirase, K. & Arai, E. (2002). Representation and planning of deformable linear object manipulation including knotting, Proc. IEEE Int. Conf. on Industrial Technology, Vol.2, pp.1321-1326, Dec.11-14, 2002

Wakamatsu, H.; Tsumaya, A.; Arai, E. & Hirai, S. (2004). Planning of one-handed knotting/raveling manipulation of linear objects, Proc. IEEE International Conference on Robotics and Automation, Vol.2, pp.1719-1725, April 26-May 1, 2004

Wu, J. Q.; Luo, Z. W.; Yamakita, M. & Ito, K. (1997). Dynamic position/force control of manipulators for contact tasks on unknown flexible plate, Trans. Japan. Soc. Mech. Eng., Vol.63, No.607, pp.937-944

Yue, S. & Henrich, D. (2002). Manipulating deformable linear objects: sensor-based fast manipulation during vibration, Proc. IEEE Int. Conf. on Robotics and Automation, Vol.3, pp.2467-2472, May11-15, 2002

Cutting Edge Robotics

Edited by Vedran Kordic, Aleksandar Lazinica and Munir Merdan

ISBN 3-86611-038-3

Hard cover, 784 pages

Publisher Pro Literatur Verlag, Germany

Published online 01, July, 2005

Published in print edition July, 2005

This book is the result of inspirations and contributions from many researchers worldwide. It presents a collection of wide range research results of robotics scientific community. Various aspects of current research in robotics area are explored and discussed. The book begins with researches in robot modelling & design, in which different approaches in kinematical, dynamical and other design issues of mobile robots are discussed. Second chapter deals with various sensor systems, but the major part of the chapter is devoted to robotic vision systems. Chapter III is devoted to robot navigation and presents different navigation architectures. The chapter IV is devoted to research on adaptive and learning systems in mobile robots area. The chapter V speaks about different application areas of multi-robot systems. Other emerging field is discussed in chapter VI - the human- robot interaction. Chapter VII gives a great tutorial on legged robot systems and one research overview on design of a humanoid robot.The different examples of service robots are showed in chapter VIII. Chapter IX is oriented to industrial robots, i.e. robot manipulators. Different mechatronic systems oriented on robotics are explored in the last chapter of the book.

How to reference

In order to correctly reference this scholarly work, feel free to copy and paste the following:

Jian Huang, Isao Todo and Tetsuro Yabuta (2005). Position / Force Hybrid Control of a Manipulator with a Flexible Tool Using Visual and Force Information, Cutting Edge Robotics, Vedran Kordic, Aleksandar Lazinica and Munir Merdan (Ed.), ISBN: 3-86611-038-3, InTech, Available from: http://www.intechopen.com/books/cutting_edge_robotics/position___force_hybrid_control_of_a_manipulator_with_a_flexible_tool_using_visual_and_force_informa

INTECH
open science | open minds

InTech Europe
University Campus STeP Ri
Slavka Krautzeka 83/A
51000 Rijeka, Croatia
Phone: +385 (51) 770 447
Fax: +385 (51) 686 166
www.intechopen.com

InTech China
Unit 405, Office Block, Hotel Equatorial Shanghai
No.65, Yan An Road (West), Shanghai, 200040, China
中国上海市延安西路65号上海国际贵都大饭店办公楼405单元
Phone: +86-21-62489820
Fax: +86-21-62489821

© 2005 The Author(s). Licensee IntechOpen. This chapter is distributed under the terms of the Creative Commons Attribution-NonCommercial-ShareAlike-3.0 License, which permits use, distribution and reproduction for non-commercial purposes, provided the original is properly cited and derivative works building on this content are distributed under the same license.